Structure Effects of Benzene Hydrogenation Studied with Sum Frequency Generation Vibrational Spectroscopy and Kinetics on Pt(111) and Pt(100) Single-Crystal Surfaces

Kaitlin M. Bratlie, Christopher J. Kliewer, and Gabor A. Somorjai*

Department of Chemistry, University of California, Berkeley, California 94720, and Materials Science Division, Lawrence Berkeley National Laboratory, Berkeley, California 94720

Received: April 28, 2006; In Final Form: June 6, 2006

Sum frequency generation (SFG) surface vibrational spectroscopy and kinetic measurements using gas chromatography have identified at least two reaction pathways for benzene hydrogenation on the Pt(100) and Pt(111) single-crystal surfaces at Torr pressures. Kinetic studies at low temperatures (310−370 K) show that benzene hydrogenation does not proceed through cyclohexene. A Langmuir−Hinshelwood-type rate law for the low-temperature reaction pathway is identified. The rate-determining step for this pathway is the addition of the first hydrogen atom to adsorbed benzene for both single-crystal surfaces, which is verified by the spectroscopic observation of adsorbed benzene at low temperatures on both the Pt(100) and Pt(111) crystal faces. Low-temperature SFG studies reveal chemisorbed and physisorbed benzene on both surfaces. At higher temperatures (370−440 K), hydrogenation of benzene to π-allyl *c*-C_6H_9 is observed only on the Pt(100) surface. Previous single-crystal studies have identified π-allyl *c*-C_6H_9 as the rate-determining step for cyclohexene hydrogenation to cyclohexane.

1. Introduction

Benzene hydrogenation is an industrially relevant reaction for several essential steps in petroleum refining and downstream chemical processing.[1] Identifying reactive surface intermediates and rate laws are key issues in understanding the mechanism of benzene hydrogenation. Furthermore, understanding how these surface intermediates and rate laws are affected by surface structure is important in extending our knowledge of single crystals to industrial catalysts.

Benzene adsorption on platinum at low pressures ($<10^{-6}$ Torr) has been studied using various surface-analytical techniques, including low-energy electron diffraction (LEED),[2] near-edge X-ray absorption fine structure spectroscopy (NEXAFS),[3] calorimetry,[4] thermal desorption spectroscopy,[5,6] electron energy loss spectroscopy (EELS),[7−9] scanning tunneling microscopy (STM),[10] and reflection−absorption infrared spectroscopy.[11,12] In addition, possible adsorption energies for different adsorption sites and surface species have been studied by density functional theory (DFT).[13−15] STM[10] and DFT[15] studies show that benzene preferentially adsorbs to bridge sites in the low coverage limit and to the threefold hollow at high coverages on the Pt(111) crystal face. The low- and high-coverage species have two distinct vibrational signatures, as studied by EELS,[8,9] which correspond to chemisorbed and physisorbed benzene. Thomas et al.[9] proposed that the chemisorbed species is a dienyl benzene, illustrated in Scheme 1a. Physisorbed benzene, on the other hand, is thought of as flat lying on the basis of NEXAFS studies.[3]

High-pressure reactions of benzene on Pt(111) have been investigated using sum frequency generation (SFG) vibrational spectroscopy[16,17] and high-pressure STM.[17] These studies observe both chemisorbed and physisorbed benzene under high-pressure conditions. STM observed small ordered regions corresponding to the *c*($2\sqrt{3} \times 3$)*rect* structure in a background of 10 Torr of benzene.[17] Between the ordered regions, individual benzene molecules were observed by STM.[17] On the basis of the SFG results, the individual molecules were assumed to be physisorbed benzene, while the ordered regions corresponded to the chemisorbed benzene. Conducting these experiments on Pt(100) will further our knowledge of this reaction, in particular how structure affects the reaction pathway.

SCHEME 1: Schematic Diagram of (a) Dienyl Chemisorbed Benzene (C_6H_6) and (b) π-allyl *c*-C_6H_9 Intermediates

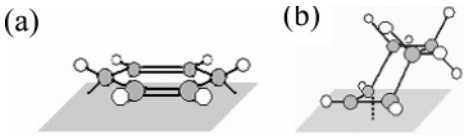

In this study, SFG vibrational spectroscopy and gas chromatography (GC) are used to investigate benzene hydrogenation at high temperatures (310−440 K) to elicit structure effect information. Media with centrosymmetry and isotropic gases do not appear in the SFG spectrum under the electric dipole approximation. Since bulk platinum has a center of inversion, its contribution to the SFG signal is negligible. The symmetry at the surface of the platinum crystal is broken, giving rise to a surface specific signal. Because the SFG signal arises solely from the adsorbates, SFG is a more sensitive tool to study interfaces than are infrared absorption and Raman spectroscopies. Electron spectroscopies typically cannot be employed under the ambient pressure conditions necessary to perform catalytic reactions.

Here, we report evidence for chemisorbed dienyl benzene (C_6H_6) as the reactive surface intermediate for benzene hydrogenation on both the Pt(100) and Pt(111) surfaces at high pressures (7.5, 10, 12.5, and 15 Torr of benzene and 10, 50, 100, and 150 Torr of H_2) and at high temperatures (310−440

* To whom correspondence should be addressed. Tel: 510-642-4053. Fax: 510-643-9668. E-mail: somorjai@socrates.berkeley.edu.

10.1021/jp062623q CCC: $33.50
Published on Web 08/19/2006

K). Both surfaces exhibit chemisorbed and physisorbed benzene coadsorbed at low temperatures. Differences arise as the temperature is increased: π-allyl c-C_6H_9 (see Scheme 1b)is observed on the Pt(100) surface at high temperatures and not on the Pt(111) surface. Previous studies show that π-allyl c-C_6H_9 is the most abundant surface intermediate during cyclohexene hydrogenation.[18,19] These studies also suggest that the hydrogenation of π-allyl c-C_6H_9 is the rate-determining step (RDS) in forming cyclohexane. Kinetic studies on benzene hydrogenation to cyclohexane at low temperatures have identified a rate law where the RDS is the addition of the first hydrogen to benzene. Herein, we discuss the temperature-, pressure-, and structure-dependent surface chemistry of benzene hydrogenation on Pt(100) and Pt(111).

2. Experimental Section

All experiments were carried out in a high-pressure/ultrahigh-vacuum (HP/UHV) system on a prepared Pt(100) or Pt(111) single-crystal surface. The HP/UHV system consists of a UHV chamber operating at a base pressure of 2×10^{-9} Torr and a high-pressure (HP) cell isolated from the UHV chamber by a gate valve. The UHV chamber is equipped with an Auger electron spectrometer (AES), a quadrupole mass spectrometer, and an Ar^+ sputter gun. Two CaF_2 conflat windows on the HP cell allow transmission of infrared (IR), visible (VIS), and sum frequency radiation for SFG experiments. The HP cell is equipped with a recirculation loop that includes a diaphragm pump and a septum for gas chromatographic analysis. The reactant and product gases are constantly mixed via a recirculation pump, while kinetic data is acquired by periodically sampling the reaction mixture and measuring the relative gas-phase composition (flame ionization detection and 0.1% AT-1000 on a Graphpac GC 80/100 packed column (Alltech)).

The Pt(100) and Pt(111) crystals were cleaned by sputtering with Ar^+ (1 keV) for 20 min, heating to 1123 K in the presence of 5×10^{-7} Torr of O_2 for 2 min, and then annealing at 1123 K for 2 min. AES and LEED were used to verify the cleanliness of the Pt(100) or Pt(111) surface after several cleaning cycles. The Pt(100) or Pt(111) sample was then transferred into the HP cell for SFG reaction studies. Benzene ($\geq$99.0%, EM Science) was purified by several freeze−pump−thaw cycles before introduction into the HP cell. Prior to the experiment, benzene was checked for impurities by means of GC. Such impurities were below 0.5% and consisted of mostly light alkanes below C_6.

SFG measurements were performed using a mode-locked Nd:YAG laser (1064 nm fundamental having a 20 ps pulse width operating at a 20 Hz repetition rate) to create a tunable IR (1800−4000 cm^{-1}) and a second harmonic VIS (532 nm) beam. The VIS beam (200 μJ) and the IR (200 μJ) beams were spatially and temporally overlapped on the Pt(111) surface with incident angles of 55 and 60°, with respect to the surface normal. All spectra were taken using a ppp polarization combination (SFG, VIS, and IR beams were all p-polarized). The generated SFG beam was sent through a monochromator, and the signal intensity was detected with a photomultiplier tube and a gated integrator as the IR beam was scanned over the frequency range of interest. The sum frequency output was normalized by the intensity of the incident infrared beam at the surface. This is necessary because gas molecules absorb some of the incoming radiation. Spectra were curve fit using a previously reported procedure[20,21] to a form of the equation

$$I_{SFG} \propto \left|\chi_{NR}^{(2)} e^{i\phi_{NR}} + \sum_q \frac{A_q}{\omega_{IR} - \omega_q + i\Gamma_q} e^{i\gamma_q}\right|^2 \qquad (1)$$

where $\chi_{NR}^{(2)}$ is the nonresonant nonlinear susceptibility, $e^{i\phi_{NR}}$ is the phase associated with the nonresonant background, A_q is the strength of the qth vibrational mode, ω_{IR} is the frequency of the incident infrared laser beam, ω_q is the frequency of the qth vibrational mode, Γ_q is the natural line width of the qth vibrational transition, and $e^{i\gamma_q}$ is the phase associated with the qth vibrational transition. Detailed descriptions on the HP/UHV system and SFG measurement can be found elsewhere.[19,22−26]

3. Results

3.1. Turnover Rates, Reaction Orders, and Arrhenius Parameters for Benzene Hydrogenation to Cyclohexane under Varied Pressures of Benzene and Hydrogen on Pt-(100) and Pt(111). Figure 1 shows the kinetic data obtained for 100 Torr of H_2 and 7.5, 10, 12.5, and 15 Torr of benzene over a range of temperatures (310−440 K). The production of cyclohexane is displayed at different temperatures by the turnover rates (TORs) [molecules·Pt site^{-1}·s^{-1}] shown in Figure 1a. The TORs are calculated on the basis of the assumption that every platinum atom is an active site. The errors associated with the measurements are shown as error bars in Figure 1a. The corresponding Arrhenius plots of the TORs are given in Figure 1b. TORs were also collected for a constant benzene pressure (10 Torr) with a varied H_2 pressure (10, 50, 100, and 150 Torr). The TORs for cyclohexane formation are shown in Figure 2a with the resultant Arrhenius plots in Figure 2b. Above 370 K, the observed TORs for cyclohexane deviate from the linear Arrhenius line; this results from a change in the surface coverage of the adsorbed species, as previously discussed.[19] Apparent activation energies and preexponentials for hydrogenation to cyclohexane are listed in Table 1. These experiments have been carried out on the Pt(111) surface previously[16] and are summarized in Table 1.

The rate law for benzene hydrogenation can be described by a standard empirical power law

$$r = k p_{C_6H_6}{}^a p_{H_2}{}^b \qquad (2)$$

where r is the rate of reaction, $p_{C_6H_6}$ and p_{H_2} are the pressures of the reactant gases (benzene and H_2, respectively), a and b are the reaction orders with respect to the reactant species, and k is the rate constant. The rate constant can be expressed as

$$k = A e^{-E_a/RT} \qquad (3)$$

where A is the preexponential factor, E_a is the activation energy, R is the gas constant, and T is temperature. The exponents a and b are determined over a range of reaction temperatures (310−370 K) using

$$a = \left[\frac{\partial \ln r}{\partial \ln p_{C_6H_6}}\right]_{p_{H2}} \qquad (4)$$

The benzene and H_2 reaction orders for cyclohexane production on both the Pt(111) and Pt(100) surfaces are listed in Table 1.

The most noticeable feature visible in Figures 1a and 2a is the sharp dip in the turnover plot at approximately 390 K. This is attributed to the onset of cyclohexene formation on the surface, resulting from a competing pathway. Cyclohexene production is observed at 370 K for benzene hydrogenation on Pt(111).[16] Cyclohexene has a larger sticking coefficient (0.2[27])

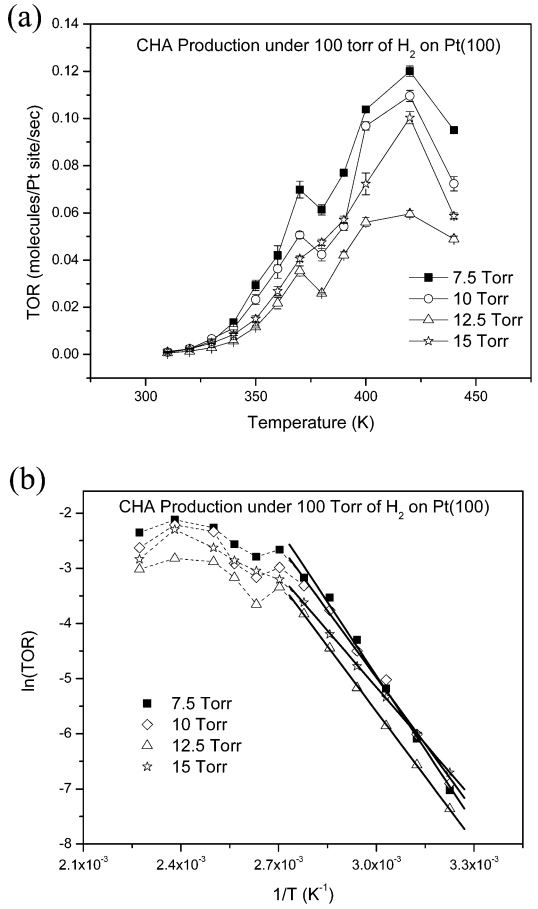

Figure 1. (a) TORs, in molecules per Pt atom per second, for benzene (7.5, 10, 12.5, and 15 Torr) in the presence of H_2 (100 Torr) on Pt(100) to form cyclohexane. (b) Arrhenius plots of the corresponding TORs. The decrease in the TOR for cyclohexane production at 380 K followed by a sharp increase at 390 K is attributed to the onset of cyclohexene production. Cyclohexene has a higher sticking probability on platinum, resulting in further hydrogenation to cyclohexane. The non-Arrhenius behavior above 370 K is explained in terms of changes in the surface coverage of the adsorbates. Apparent activation energies and preexponentials are listed in Table 1. Dotted lines were drawn as visual aids.

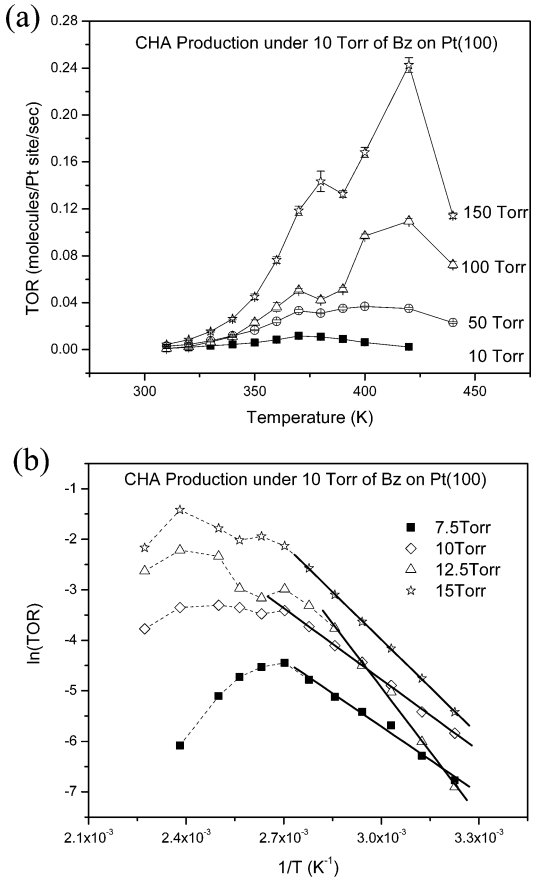

Figure 2. (a) TORs, in molecules per Pt atom per second, for benzene (10 Torr) in the presence of H_2 (10, 50, 100, and 150 Torr) on Pt(100) to form cyclohexane. (b) Arrhenius plots of the corresponding TORs. The decrease in the TOR for cyclohexane production at 380 K followed by a sharp increase at 390 K is attributed to the onset of cyclohexene production. Cyclohexene has a higher sticking probability on platinum, resulting in further hydrogenation to cyclohexane. The non-Arrhenius behavior above 370 K is explained in terms of changes in the surface coverage of the adsorbates. Apparent activation energies and preexponentials are listed in Table 1. Dotted lines were drawn as visual aids.

than cyclohexane (<0.1[4]) on Pt(111), which allows the gas-phase precursor to remain on the surface and further hydrogenate.[16] We presume that adsorbed cyclohexene is formed on Pt(100) during the reaction at high temperatures on the basis of these results.

3.2. Temperature Dependence of the Major Surface Species under Varied Pressures of Benzene and Hydrogen on Pt(100) and Pt(111): SFG Vibrational Spectroscopy Results and Peak Assignments. Figure 3 shows the SFG spectra of the surface species present on Pt(100) at 15 Torr of benzene and 100 Torr of H_2 at various temperatures. At 300 K, three peaks are observed at 2945, 3030, and 3060 cm^{-1}. The mode at 3060 cm^{-1} decreases in intensity as the temperature is increased and disappears completely at 380 K. This peak has been previously identified by SFG[16] and EELS[9] as the aromatic C−H stretch of the physisorbed benzene. The intensity of the peak at 3030 cm^{-1} neither increases nor decreases as the temperature is increased. This mode is also present on the Pt-(111) surface and is assigned by SFG[16] to the vinylic stretch of a dienyl chemisorbed benzene (see Scheme 1a). The mode at 2945 cm^{-1} is also observed on the Pt(111) surface and assigned to the sp^3 hybridized C−H stretch of the dienyl chemisorbed benzene. Dienyl chemisorbed benzene is composed of four single and two double carbon−carbon bonds. The two singly bound carbon atoms are also bound to the platinum surface, giving rise to the sp^3 hybridization character in the spectral signature. Unlike the Pt(111) surface, the peaks at 2945 and 3030 cm^{-1} do not simultaneously grow and decay with temperature variations. Furthermore, the peak at 2945 cm^{-1} red shifts to 2940 cm^{-1} as the temperature is increased, and a new peak appears at 2865 cm^{-1}. It becomes clear by comparison that the SFG spectra in Figure 3 are similar to previous SFG data of π-allyl c-C_6H_9 on Pt(100).[19] The SFG[19] spectrum of π-allyl c-C_6H_9 on Pt(100) is characterized by two peaks at υ_{sym}-(CH_2) = 2865 and $\upsilon_{asym}(CH_2)$ = 2940 cm^{-1}, with the υ_{asym}-(CH_2) peak being approximately twice as intense as the $\upsilon_{sym}(CH_2)$ peak. Hence, the modes in Figure 3 are assigned as follows: $\upsilon_{sym}(CH_2)$ = 2865 cm^{-1}, $\upsilon_{asym}(CH_2)$ = 2940 cm^{-1}, υ(H−C−C−) = 2945 cm^{-1}, υ(C−H)(vinylic) = 3030 cm^{-1}, and υ(C−H)(aromatic) = 3060 cm^{-1}. Cooling the platinum surface temperature from 440 to 300 K reveals the reversible behavior of the surface composition.

The same surface species are present at other pressure combinations (7.5 and 12.5 Torr of benzene under 100 Torr of H_2 and 10 Torr of benzene under 10, 50, 100, and 150 Torr of H_2) on the Pt(100) surface. Both chemisorbed and physisorbed benzene are coadsorbed at 300 K. Heating the crystal surface to 340 K forms π-allyl c-C_6H_9 on the surface, which is

TABLE 1: Pre-exponentials (in molecules per Pt atom per second), Apparent Activation Energies (in kcal/mol), Orders for Both H_2 and Benzene, Isokinetic Temperature (in K), and the Critical Vibration (in cm^{-1}) for Cyclohexane Production under a Constant Pressure of 10 Torr of Benzene while Varying H_2 and under a Constant Pressure of 100 Torr of H_2 while Varying Benzene on Pt(111)[16] and Pt(100)

	Pt(111)		Pt(100)	
	ln(A/molecules site^{-1} s^{-1})	E_a/(kcal mol^{-1})	ln(A/molecules site^{-1} s^{-1})	E_a/(kcal mol^{-1})
		10.5 Torr benzene		
11.2 Torr H_2	3.0 ± 0.3	7.0 ± 0.2	5.4 ± 0.8	8.7 ± 0.5
52 Torr H_2	4.7 ± 0.5	8.0 ± 0.3	6.3 ± 0.3	9.4 ± 0.2
105 Torr H_2	7.3 ± 0.1	9.8 ± 0.1	14.9 ± 0.2	15.7 ± 0.1
158 Torr H_2	8.5 ± 0.7	10.6 ± 0.4	11.2 ± 0.1	12.5 ± 0.1
		105 Torr H_2		
7.9 Torr Bz	6.0 ± 0.3	9.3 ± 0.3	20.0 ± 0.2	18.9 ± 0.1
10.5 Torr Bz	7.3 ± 0.1	9.8 ± 0.1	17.1 ± 1.2	16.8 ± 0.8
13.3 Torr Bz	5.9 ± 0.1	8.9 ± 0.1	14.9 ± 0.2	15.7 ± 0.1
16.5 Torr Bz	8.1 ± 0.7	10.5 ± 0.2	12.4 ± 0.2	13.6 ± 0.1
		order Pt(111)		order Pt(100)
benzene		−1.1 ± 0.1		−1.1 ± 0.3
H_2		0.6 ± 0.01		0.6 ± 0.02
		T_i/(K)		ν/(cm^{-1})
cyclohexane		358 ± 5		501 ± 7

coadsorbed with physisorbed and chemisorbed benzene. Further increasing the temperature to 380 K desorbs the physisorbed benzene, leaving π-allyl c-C_6H_9 and chemisorbed benzene on the surface. Cooling the surface reverses the reaction, resulting in physisorbed benzene being the dominant surface species.

Figure 4 shows the SFG spectra of the surface species present on Pt(111) under 10 Torr of benzene and 10 Torr of H_2 at varied temperatures. Much like the benzene hydrogenation on Pt(100), the spectrum at 300 K exhibits three peaks at 2945, 3030, and 3060 cm^{-1}. These three peaks represent physisorbed and dienyl chemisorbed benzene. As the surface temperature is increased to 380 K, the physisorbed benzene desorbs. The two peaks that are assigned to the dienyl chemisorbed benzene simultaneously increase in intensity as the surface temperature is increased to 420 K. On the basis of these peaks growing and decaying in unison as the temperature is varied coupled with the notable absence of a $\nu_{sym}(CH_2)$ peak, we conclude that π-allyl c-C_6H_9 is not present on the Pt(111) surface. Cooling the surface reveals that, like that on Pt(100), the benzene hydrogenation reaction is reversible on Pt(111).

4. Discussion

4.1. Langmuir−Hinshelwood Mechanism and Suggested Reaction Pathways for Benzene Hydrogenation to Cyclohexane on Pt(111) and Pt(100). The reaction orders found in Table 1 for the hydrogenation of benzene on both Pt(111) and Pt(100) corresponds to a Langmuir−Hinshelwood-type mechanism where the RDS is the surface reaction between an adsorbed benzene molecule and one adsorbed hydrogen atom. The proposed mechanism for benzene hydrogenation to cyclohexane involves the following elementary reaction steps:

$$H_2 + 2* \underset{}{\overset{K_{H_2}}{\rightleftharpoons}} 2H* \qquad \text{(R1)}$$

$$C_6H_6 + * \underset{}{\overset{K_1}{\rightleftharpoons}} C_6H_6* \qquad \text{(R2)}$$

$$C_6H_6* + H* \xrightarrow{k_2} C_6H_7* + * \qquad \text{(R3)}$$

According to Saeys et al.,[14] C_6H_6* is the most stable adsorbed C_6 species in the conversion of benzene to cyclohexane. This choice of RDS is in agreement with the spectroscopic evidence that shows only adsorbed benzene present on both the Pt(111) and Pt(100) crystal surfaces at low temperatures. The rate of benzene hydrogenation to cyclohexane can be written as

$$r_{C_6H_6} = k_2\theta_{C_6H_6*}\theta_{H*} \qquad (5)$$

where the coverage of adsorbed hydrogen, θ_{H*}, is determined from the equilibrium of gas-phase H_2 and adsorbed hydrogen,

$$\theta_{H*} = \sqrt{K_{H_2}p_{H_2}}\,\theta_* \qquad (6)$$

where p_{H_2} is the pressure of the gas-phase H_2. The coverage of benzene, $\theta_{C_6H_6*}$, is also determined by the equilibrium of gas-phase benzene and adsorbed benzene,

$$\theta_{C_6H_6*} = K_1 p_{C_6H_6}\theta_* \qquad (7)$$

where $p_{C_6H_6}$ is the pressure of gas-phase benzene. Inserting eqs 6 and 7 into eq 5 results in

$$r_{C_6H_6} = k_2K_1\sqrt{K_{H_2}}p_{C_6H_6}\sqrt{p_{H_2}} \qquad (8)$$

The site balance for the system is given by

$$1 = \theta_* + \theta_{C_6H_6*} + \theta_{H*} \qquad (9)$$

which leads to a Langmuir−Hinshelwood-type rate expression for benzene hydrogenation to cyclohexane,

$$r_{C_6H_6} = \frac{k_{app}p_{C_6H_6}\sqrt{p_{H_2}}}{(1 + K_1p_{C_6H_6} + \sqrt{K_{H_2}p_{H_2}})^2} \qquad (10)$$

where $k_{app} = K_1k_2\sqrt{K_{H_2}}$. The rate expression allows the order of benzene to vary from −1 to first-order and the order of H_2 to vary from −1/2 to half-order. Since benzene adsorption at low temperatures (300 K ≤ T ≤ 400 K) is favorable and there is a high gas-phase pressure of benzene, $K_1p_{C_6H_6}$ is much larger

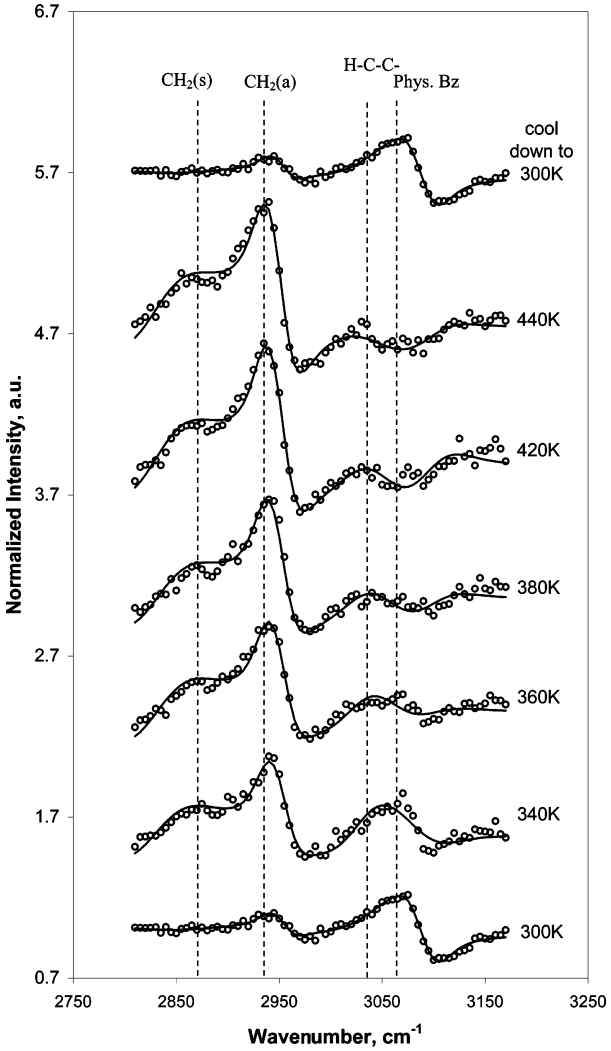

Figure 3. Temperature-dependent SFG spectra of surface species on Pt(100) under 15 Torr of benzene and 100 Torr of H_2 in the range of 300−440 K. The top SFG spectrum was taken after the metal surface was cooled from 440 to 300 K. CH_2(s), CH_2(a), vinylic (H−C═C−), and physisorbed benzene (phys. Bz) bands are identified. Markers represent experimental data, and solid lines represent the curve fits.

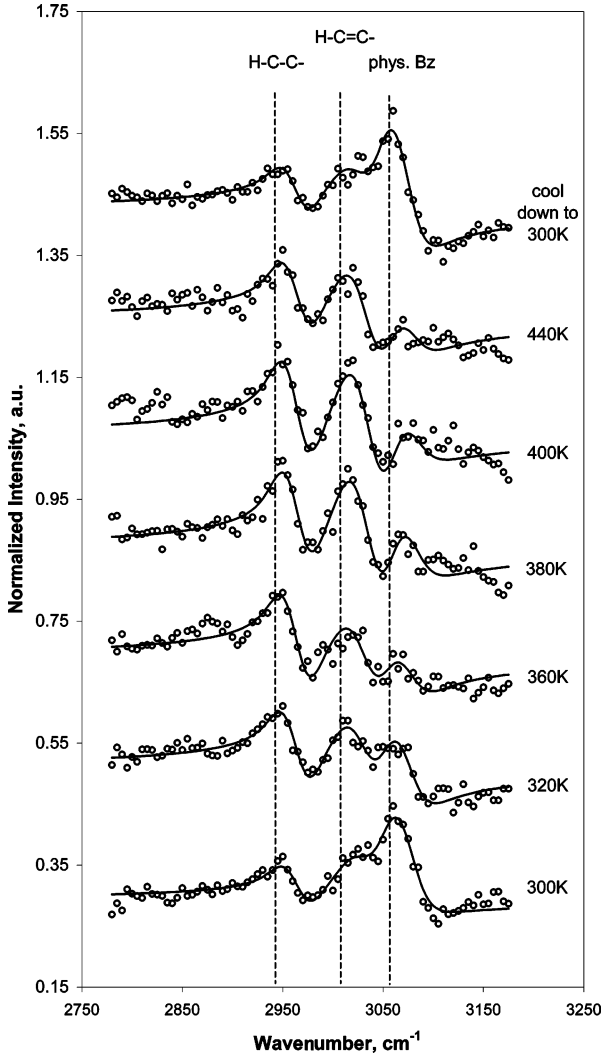

Figure 4. Temperature-dependent SFG spectra of surface species on Pt(111) under 10 Torr of benzene and 10 Torr of H_2 in the range of 300−440 K. The top SFG spectrum was taken after the metal surface was cooled from 440 to 300 K. H−C−C−, vinylic (H−C═C−), and physisorbed benzene (phys. Bz) bands are identified. Markers represent experimental data, and solid lines represent the curve fits.

than $1 + \sqrt{K_{H_2} p_{H_2}}$, and the rate expression becomes

$$r_{C_6H_6} = \frac{k_{app}\sqrt{p_{H_2}}}{K_1^2 p_{C_6H_6}} \qquad (11)$$

This low-temperature rate expression shows the dependence on benzene is −1, and for hydrogen it is half-order, which are strikingly similar to the experimentally obtained reaction orders listed in Table 1 for both Pt(111) and Pt(100). The theoretical rate expression in eqs 10 and 11 were verified by fitting to the experimentally obtained rates.

Previous reaction studies of benzene hydrogenation on Pt(111) concluded that at least two reaction pathways exist since gas-phase cyclohexene evolves only at high temperatures.[16] Furthermore, a decrease and sudden increase in turnover at 370 K coincides with the onset of cyclohexene formation and, hence, another reaction pathway. A similar trend is presumed to also occur on the Pt(100) surface since the turnover plots display features similar to those of Pt(111). Sayes et al.[14] developed a possible reaction pathway by DFT that does not proceed through cyclohexene, as the experimental data implies. The proposed reaction pathway occurs in a Horiuti−Polanyi scheme[28] that adds hydrogens to benzene adsorbed to the platinum surface in an ortho fashion. Saeys et al.[14] also found that "the thermodynamic sink of the energy profile is clearly the adsorbed benzene and hydrogen. They are likely to be the most-abundant reaction intermediates." Again, this pathway is consistent with the spectral evidence showing only adsorbed benzene at low temperatures and the rate expression that arises from the addition of the first hydrogen.

One of the reaction pathways at higher temperatures is the hydrogenation of cyclohexene to cyclohexane. Previous investigations into this reaction by Bratlie et al.[19] on the Pt(100) surface and by Yang et al.[18] on the Pt(111) surface identified π-allyl c-C_6H_9 as the most abundant reactive intermediate and its hydrogenation as a likely RDS for cyclohexene hydrogenation. The spectrum in Figure 3 clearly shows π-allyl c-C_6H_9 on the Pt(100) surface in the presence of benzene; however, π-allyl c-C_6H_9 is not visible on the Pt(111) surface. This indicates that adsorbed cyclohexene more readily dehydrogenates to form π-allyl c-C_6H_9 on the Pt(100) surface than on the Pt(111) surface.

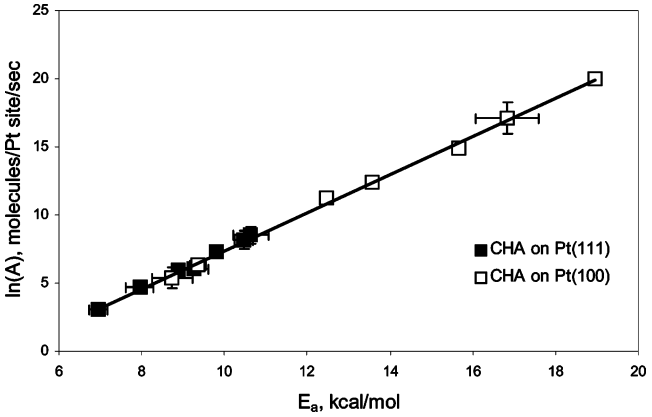

Figure 5. Constable plot for the hydrogenation of benzene to cyclohexane on Pt(111) and Pt(100).

4.2. Compensation Effect and Isokinetic Temperature. The apparent activation energies and preexponential factors for all pressure combinations on both the Pt(100) and Pt(111) surfaces are listed in Table 1. Plotting these Arrhenius parameter pairs forms a straight line, presented in Figure 5, which is attributed to the compensation effect. Taking the natural logarithm of eq 3 yields

$$\ln A = \frac{E_a}{RT} + \ln k \tag{12}$$

On the basis of eq 12, the slope of Figure 5 is related to the isokinetic temperature (T_{iso}). For cyclohexane formation on both Pt(100) and Pt(111), T_{iso} is 358 ± 5 K, which corresponds reasonably well with the temperature at which the Arrhenius plots intersect. Possible explanations for the compensation effect have been explored extensively and have been reviewed by Bond et al.[29] One of the interpretations of the isokinetic temperature cited by Bond et al.[29] is a model proposed by Larsson,[30] which assumes there is a transfer of "energy into the vibrational mode of the reactant that most effectively takes the system to the activated site" from the active site. On the basis of this model, Larsson[30] derives the following equation:

$$T_{iso} = \frac{Nhc}{2R\upsilon} = 0.719\upsilon \tag{13}$$

where υ is the vibrational mode leading toward reaction, N is Avogadro's number, h is Planck's constant, and c is the speed of light. Using eq 13 to interpret T_{iso} in terms of wavenumbers, the critical frequency of vibration is 501 ± 7 cm^{-1}. Difficulties arise in assigning this critical vibration to an adsorbed surface species. Thomas et al.[9] found that physisorbed and chemisorbed benzene both exhibit Pt−C stretches at 550 and 475 cm^{-1}, respectively. Lamont et al.[31] reported a ring deformation for cyclohexene at 539 cm^{-1} and a CCC deformation for cyclohexane at 515 cm^{-1}. These are just three of the possible adsorbed molecules that may be present on the platinum surface, illustrating how the critical vibration could belong to any number of adsorbed C_6 surface species.

5. Conclusions

The low-temperature reaction pathway for benzene hydrogenation has been clarified through kinetic measurements, SFG vibrational spectroscopy, and parameters obtained from fits to the experimentally determined TORs on both the Pt(100) and Pt(111) single-crystal surfaces. A Langmuir−Hinshelwood-type rate expression for the low-temperature reaction pathway was identified, and its RDS is the addition of the first hydrogen to adsorbed benzene. The rate expression was experimentally verified by the reaction orders for benzene and hydrogen obtained from kinetic measurements and by SFG measurements. At 300 K, physisorbed and chemisorbed benzene were observed on both single-crystal surfaces. Increasing the temperature desorbed the physisorbed benzene from both surfaces and produced π-allyl c-C_6H_9 on the Pt(100) surface only. Heating the single-crystal surfaces to 440 K and subsequently cooling them to 300 K resulted in SFG spectra that were identical to those obtained before reaction, indicating complete reversibility of the surface composition for both Pt(100) and Pt(111). Chemisorbed benzene was determined to be the reactive surface intermediate responsible for the RDS in the Langmuir−Hinshelwood-type rate expression. On the basis of previous studies, π-allyl c-C_6H_9 was concluded as the RDS in cyclohexene hydrogenation on both platinum crystal surfaces, a reaction that occurs at higher temperatures.

Acknowledgment. This work was supported by the Director, Office of Energy Research, Office of Basic Energy Sciences, and Materials Science Division of the U.S. Department of Energy under Contract DE-AC02-05CH11231.

References and Notes

(1) Cooper, B. H.; Donnis, B. B. L. *Appl. Catal. A* **1996**, *137*, 203.
(2) Ogletree, D. F.; Van Hove, M. A.; Somorjai, G. A. *Surf. Sci.* **1987**, *183*, 1.
(3) Horsley, J. A.; Stohr, J.; Hitchcock, A. P.; Newbury, D. C.; Johnson, A. L.; Sette, F. *J. Chem. Phys.* **1985**, *83* (12), 6099.
(4) Ihm, H.; Ajo, H. M.; Gottfried, J. M.; Bera, P.; Campbell, C. T. *J. Phys. Chem. B* **2004**, *108* (38), 14627.
(5) Lutterloh, C.; Biener, L.; Pohlmann, K.; Schenk, A.; Kuppers, J. *Surf. Sci.* **1996**, *352*−*354*, 133.
(6) Tsai, M.-C.; Muetterties, E. L. *J. Am. Chem. Soc.* **1982**, *104*, 2534.
(7) Abon, M.; Bertolini, J. C.; Billy, J.; Massardier, J.; Tardy, B. *Surf. Sci.* **1985**, *162*, 395.
(8) Lehwald, S.; Ibach, H.; Demuth, J. E. *Surf. Sci.* **1978**, *78*, 577.
(9) Thomas, F. S.; Chen, N. S.; Ford, L. P.; Masel, R. I. *Surf. Sci.* **2001**, *486*, 1.
(10) Weiss, P. S.; Eigler, D. M. *Phys. Rev. Lett.* **1993**, *71* (19), 3139.
(11) Haq, S.; King, D. A. *J. Phys. Chem.* **1996**, *100*, 16957.
(12) Haaland, D. M. *Surf. Sci.* **1981**, *102*, 405.
(13) Saeys, M.; Reyniers, M.; Marin, G. B.; Neurock, M. *Surf. Sci.* **2002**, *513*, 315.
(14) Saeys, M.; Reyniers, M.; Marin, G. B. *J. Phys. Chem. B* **2002**, *106*, 7489.
(15) Morin, C.; Simon, D.; Sautet, P. *J. Phys. Chem. B* **2004**, *108*, 5653.
(16) Bratlie, K. M.; Flores, L. D.; Somorjai, G. A. *J. Phys. Chem. B* **2006**, *110*, 10051.
(17) Bratlie, K. M.; Montano, M. O.; Flores, L. D.; Paajanen, M.; Somorjai, G. A. *J. Am. Chem. Soc.*, submitted for publication, 2006.
(18) Yang, M.; Chou, K. C.; Somorjai, G. A. *J. Phys. Chem. B* **2003**, *107*, 5267.
(19) Bratlie, K. M.; Flores, L. D.; Somorjai, G. A. *Surf. Sci.* **2005**, *599* (1−3), 93.
(20) Bain, C. D.; Davies, P. B.; Ong, T. H.; Ward, R. N.; Brown, M. A. *Langmuir* **1991**, *7*, 1563.
(21) Moore, F. G.; Becraft, K. A.; Richmond, G. L. *Appl. Spectrosc.* **2002**, *56*, 1575.
(22) Kung, K. Y.; Chen, P.; Wei, F.; Rupprechter, G.; Shen, Y. R.; Somorjai, G. A. *Rev. Sci. Instrum.* **2001**, *72*, 1806.
(23) Yang, M.; Tang, D. C.; Somorjai, G. A. *Rev. Sci. Instrum.* **2003**, *74*, 4554.
(24) Shen, Y. R. *The Principles of Nonlinear Optics*; Wiley: New York, 2003.
(25) Shen, Y. R. *Annu. Rev. Phys. Chem* **1989**, *40*, 327.
(26) Shen, Y. R. *Nature* **1989**, *337*, 519.
(27) Henn, F. C.; Diaz, A. L.; Bussel, M. E.; Huggenschmidt, M. B.; Domagala, M. E.; Campbell, C. T. *J. Phys. Chem.* **1992**, *96*, 5965.
(28) Horiuti, J.; Polanyi, M. *Trans. Faraday Soc.* **1934**, *30*, 1164.
(29) Bond, G. C.; Keane, M. A.; Kral, H.; Lercher, J. A. *Catal. Rev.* **2000**, *42* (3), 323.
(30) Larsson, R. *Catal. Today* **1987**, *1*, 93.
(31) Lamont, C. L. A.; Borbach, M.; Marin, R.; Gardner, P.; Jones, T. S.; Conrad, H.; Bradshaw, A. M. *Surf. Sci.* **1997**, *374*, 215.